REFERENCES

[1] R. Kolluru, K. P. Valavanis, and T. Hebert, "Modeling, analysis and performance evaluation of a robotic gripper for limp material handling," *IEEE Trans. Syst., Man, Cybern.*, vol. 20, pp. 480–48, 1998.

[2] T. Hebert, K. P. Valavanis, and R. Kolluru, "A real-time hierarchical sensor-based robotic system architecture," *J. Intell. Robotic Syst.*, vol. 7, pp. 1–27, 1997.

[3] J. E. Shigley, *Engineering Design*, 3rd ed. New York: MacGraw-Hill Series in Mechanical Engineering, 1977.

[4] W. T. Thomson, *Theory of Vibration with Applications*, 3rd ed. Englewood Cliffs, NJ: Prentice-Hall, 1988.

[5] D. Dubois and H. Prade, *Fuzzy Sets and Systems: Theory and Applications*. New York: Academic, 1980.

[6] D. Driankov, H. Hellendoorn, and M. Reinfrank, *Introduction to Fuzzy Control*. New York: Springer-Verlag, 1996.

[7] *Fuzzy Logic Toolbox User's Guide*. Natick, MA: The Math Works, Inc., 1998.

[8] W. S. Janna, *Introduction to Fluid Mechanics*. Boston, MA: PWS Eng., 1987.

[9] P. N. Modi and S. M. Seth, *Hydraulic and Fluid Mechanics*, 10th ed. New Delhi, India: Standard Book House, 1991.

[10] N. C. Tsourveloudis, R. Kolluru, and K. P. Valavanis, "Fuzzy control of suction-based robotic gripper systems," presented at the 1998 IEEE Int. Conf. Control Applicat., Trieste, Italy.

[11] M. H. Lawry, I-DEAS Master Series Mechanical CAE/CAD/CAM Software, Structural Dynamics Research Corporation (SDRC), OH, 1993.

[12] N. C. Tsourveloudis, R. Kolluru, K. P. Valavanis, and D. Gracanin, "Suction Control of a Robotic Gripper: A Neuro-Fuzzy Approach," *J. Intell. Robotic Syst.*, vol. 9, pp. 1–21, 1999.

Mobile Robot Navigation in 2-D Dynamic Environments Using an Electrostatic Potential Field

Kimon P. Valavanis, Timothy Hebert, Ramesh Kolluru, and Nikos Tsourveloudis

***Abstract*—This paper proposes a solution to the two-dimensional (2-D) collision free path planning problem for an autonomous mobile robot utilizing an electrostatic potential field (EPF) developed through a resistor network, derived to represent the environment. No assumptions are made on the amount of information contained in the a priori environment map (it may be completely empty) and on the shape of the obstacles. The well-formulated and well-known laws of electrostatic fields are used to prove that the proposed approach generates an approximately optimal path (based on cell resolution) in a real-time frame. It is also proven through the classical laws of electrostatics that the derived potential function is a global navigation function (as defined by Rimon and Koditschek [11]), that the field is free of all local minima and that all paths necessarily lead to the goal position. The complexity of the EPF generated path is shown to be $O(mn_M)$, where m is the total number of polygons in the environment and n_M is the maximum number of sides of a polygonal object. The method is tested both by simulation and experimentally on a Nomad200 mobile robot platform equipped with a ring of sixteen sonar sensors.**

***Index Terms*—Electrostatic potential field, mobile robots, navigation.**

Manuscript received August 15, 1998; revised November 20, 1999. This work supported in part by NSF Grants BES-9506771 and BES-9712565. This paper was recommended by Associate Editor R. A. Hess.

K. P. Valavanis, T. Hebert, and R. Kolluru are with the Robotics and Automation Laboratory, The Center for Advanced Computer Studies, University of Louisiana Lafayette, Lafayette, LA 70504 USA.

N. Tsourveloudis was with the Robotics and Automation Laboratory, The Center for Advanced Computer Studies, University of Louisiana Lafayette, Lafayette, LA 70504 USA. He is now with the Department of Production Engineering and Management, Technical University of Crete, 73100 Chania, Greece.

Publisher Item Identifier S 1083-4427(00)01727-6.

I. INTRODUCTION

This paper proposes an Electrostatic Potential Field (EPF) based solution to the Mobile Robot (MR) path planning and collision avoidance problem in two-dimensional (2-D) dynamic environments. The EPF is obtained in four steps:

1) create an *occupancy map* of the environment;
2) create the corresponding *resistor network* that is representative of the MR's operational environment;
3) create the *conductance map* from the resistor network;
4) solve the resistor network to obtain the *potential field*.

The laws of electrostatic fields are used to prove that the proposed approach generates in real-time a local minima free *minimum occupancy* approximately optimal path, and that all generated paths necessarily lead to the goal position. No assumptions are made on the amount of information contained in the environment *a priori* map; the map may be (initially) completely empty. However, a complete sensor based model of the environment is built and information from environment maps is combined with on-line sonar sensor data, to plan, replan and execute a collision free path in real-time. The resolution of the environment map depends on the "size" of the smallest possible square cell in the grid. The MR is modeled as a "point" about its center of mass; hence, the 2-D workspace and the configuration space coincide. The MR is treated as a "point source" where current is injected into it to compute the adjacent cell resistances. Further, no assumptions are made on the shape of obstacles, their location and their velocities. Obstacles are stored as a collection of line segments with their half-planes intersecting to form the obstacle area. Obstacles are modeled as areas of high resistance within an area of low resistance; thus, areas of high obstacle occupancy are mapped to high resistances and areas containing relatively few obstacles are mapped to low resistances. Completely occupied cells of the network are modeled as an infinite resistance (open circuit). The cell the robot is assigned to is treated as an "empty cell" with no object, so the robot may move through and out of the cell. With a maximum potential at the robot's initial position and the sole minimum at the desired goal point, an EPF is created in which most of the current flow is in areas of (least) minimum resistance, corresponding to a path of minimum occupancy in the real environment while moving to the goal point. Stated differently, the optimum path minimizes the sum of swept occupancies (the total swept occupancy); the MR is pushed away from the boundary of obstacles while being attracted towards the goal position. It is shown that the complexity of the EPF generated path is linear with respect to the number of obstacle edges within the environment, $O(mn_M)$, where m is the total number of polygons in the environment and n_M is the maximum number of sides of a polygonal object.

The rest of the paper is organized as follows: Section II summarizes related work and discusses the fundamental laws of electrostatic potential fields, used as justification for the proposed solution. Section III presents the path planner solution, Section IV identifies similarities of the proposed approach with dynamic programming, and Section V presents simulation and real-time results. Section VI concludes the paper.

II. RELATED WORK AND BACKGROUND INFORMATION

A. Related Work

Most solution approaches to the MR navigation problem recommend global navigation (generating a path leading to the goal point) and local navigation (follow the global path avoiding collisions with obstacles). A survey of techniques used for navigational planning along with a

comprehensive study of the problem is given in [39]. Global planners may be classified into roadmaps (visibility graphs, Voronoi diagrams, freeway net, and silhouette) [19]–[25], exact and approximate cell decomposition approaches [26]–[29], and artificial potential fields (APF's). APF approaches generate a collision-free path from the field formed by the obstacles and the goal point in the robot workspace [7], [9]–[12]. Proposed solutions to overcome the problem of local minima may be found in [8], [11], [13], [16]–[18], [32]. Several researchers have also used the actual EPF [31], [36], [37], or even the magnetic field [35] to solve a specific problem. In most cases a resistor network is created as a hardware-based, analogue solution to a set of equations. A comprehensive list of related references and a comparative study of pertinent approaches including computational complexity comparisons may be found in [12] and [16].

B. Background Information

Gauss's law states that the total outward flux of the electric field intensity over any closed surface S in free space equals the total charge enclosed in the surface Q_S divided by the permittivity of free space ε. Further, the curl-free electrostatic field $\mathbf{E}$ is the gradient of the vector potential field ϕ. Combining Gauss's law with the definition of electrostatic potential results in

$$\nabla \cdot E = \nabla \cdot (\nabla \phi) = \nabla^2 \phi = \frac{Q_S}{\varepsilon} \tag{1}$$

where Q_S is the free charge in the Gaussian surface. In a closed system, the only free charge is provided by external sources. At points of the system that do not include sources the second derivative is equal to zero, and Laplace's equation is satisfied. Therefore, no minimum or maximum is located internal to the field. At a source (sink), Q_S is positive (negative) thus, a maximum (minimum) exists [1], [2].

Considering an arbitrary volume V bounded by surface S and with a net charge Q within this region, it is known that the current I leaving the region is the total outward flux of the current density vector through the surface S

$$I = \oint_S D \cdot ds = -\frac{dQ}{dt} = -\frac{d}{dt} \int_V \rho \cdot dv \tag{2}$$

where D is the volume current density and ρ is the charge density. For a stationary volume

$$\int_V \nabla \cdot D \; dv = -\int_V \frac{\partial \rho}{\partial t} \, dv \quad \text{or} \quad \nabla \cdot D = -\frac{\partial \rho}{\partial t}. \tag{3}$$

For steady currents, charge density does not vary with time, $\nabla \cdot D = 0$. Over any closed surface, the above equation results in an expression of Kirchhoff's Current Law (KCL)

$$\oint_S D \cdot ds = 0 \Rightarrow \sum_j I_j = 0. \tag{4}$$

Given a network of resistors, define $K = 1 \; \cdots \; N$as the set of all nodes of the network. Each node of the network has a number of resistors centrally tied. The actual number of resistors is determined by the connectivity of the network. Let G be an $N \times 1$ matrix with g_k the conductance of each resistor of node $k \in K$. In matrix form the complete system of equations is $A \cdot V = J$ where A is an $N \times N$ matrix and V and J are $N \times 1$ matrices. The matrix V is the potential of each node in the resistor network, J is the matrix of external current sources connected to the network, and A is the system matrix. To obtain A, KCL is applied to each node of the resistor network

$$\sum_{k \in K_l} I_{lk} = j_l \quad \forall \, l \in K. \tag{5}$$

$K_l \subseteq K$ is the set of all nodes connected to node l; I_{lk} is the current of the branch between nodes l and k; and j_l is the total current from external current sources entering node l. By replacing each branch current, I_{lk}, with its equivalent statement as defined by Ohm's Law, g_{lk} being the conductance of the branch connected to the lth and kth nodes (with l the central node of scrutiny), one gets

$$\sum_{k \in K} g_{lk}(v_1 - v_k) = j_l. \tag{6}$$

$(v_l - v_k)$ is the potential drop from l to k, and $g_{lk} = (g_l \cdot g_k / g_l + g_k)$, $g_{kl} = g_{lk}, \forall \{k, l\} \in K$.

It is proven in [3] and [4] that *the current in a network of linear passive resistors distributes itself in such a manner that the network settles into a unique state of minimum power dissipation*. The unique solution to the resistor network system of equations is equivalent to minimizing the instantaneous power consumed by the network and yields a maximum current path that follows the path of least resistance. The potential field created over a continuous surface, and through a discrete network of linear passive resistors, is shown to be free of all local minima, except at places of external sources or sinks.

III. The Proposed Solution

The navigation problem may be compared to the flow of electric current within a sheet of conducting material. The proposed solution implements a discrete form of the comparison, mapping obstacles into a discrete resistor network. Through a combination of serial and parallel resistances, the representational resistance matrix reduces to a finite number of paths directly proportional to the number of objects in the field. Each path has its head at the highest potential, and its tail at the lowest potential corresponding to the initial and goal positions of the MR, respectively. The path following the steepest gradient from the initial position to the goal position will be the path of least resistance, forming a minimal occupancy path from the initial position to the goal position.

Four major modules: 1) *Object Detection*, 2) *Localization*, 3) *Path Planning*, and 4) *Collision Avoidance* perform all tasks, while the sensor based environment map generation and trajectory following are being inherently included in the four mentioned modules [16]. The algorithm to create the potential field follows four steps:

Step 1) Create an *occupancy map* of the environment
Step 2) Create the *resistor network*
Step 3) Create the *conductance map*
Step 4) Solve the resistor network to obtain the *potential field*.

A. The Occupancy Map

The potential field is actually used to calculate the path, however cell decomposition is used to create the environment map. The space in which the navigation takes place is first mapped onto a regular grid. *Level mapping* and *binary mapping* is used to map the object into the occupancy map. Fig. 1 shows, imposed on an object, the regular grid used to perform the mapping into the occupancy map.

Both binary and level mapping are needed in a navigation approach. In a global path planner, the resistor network must be able to scale the mapping from the environment to the network so that the goal point is included in the field. If the distance to the goal point is large, one cell may map into a large physical area. If obstacles are smaller than the cell size, a binary mapping technique is more likely to be unable to find a path to the goal since it marks a single cell, which may only be minimally occupied, as full. In this instance, if a level mapping technique is used, a minimally occupied cell is marked as such and the robot is allowed to pass through the cell. The local collision avoidance must not allow the robot to attempt to move through an occupied area;

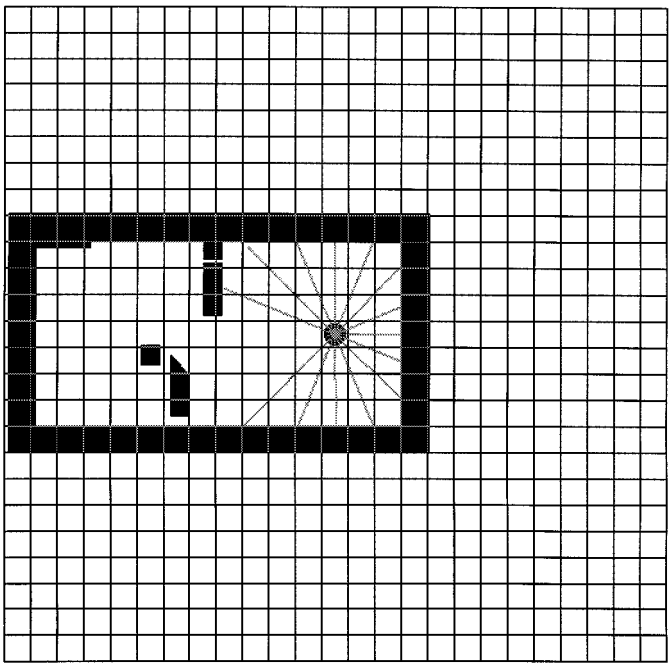

Fig. 1. Creation of the occupancy map. The robot is the circle. Sonar readings are represented as lines radiating from the robot. For the *Nomad200*, new sonar readings are obtained every 0.6 s.

thus, a binary mapping is required so that a physical area close to the robot is rendered impassable by the presence of any object. Cells that are close to the robot are mapped from the environment to the resistor network using a binary technique; while more distant cells are mapped according to the percentage occupancy of the cell—the level mapping technique.

B. The Resistor Network and the Conductance Map

Once the occupancy map is generated, each cell is then mapped onto a resistor network by replacing each cell in the occupancy map with a set of eight resistors (N, NE, E, SE, S, SW, W, NW), each resistor connected at a central point. The resistor network is obtained using the $\propto$-norm approach. Each resistor is connected to one resistor from the eight neighboring cells, unless the cell is on the boundary, in which case those resistors on the outer edge(s) are left open circuited (infinite resistance).

The value of the resistors is determined by the value of the corresponding cell in the occupancy map as shown in Fig. 2 and by the function of (7). Fig. 2 shows the sample resistance (heuristically determined) mapping function [16] utilized to map the occupancy of a cell into the conductivity of a node in the resistor network. Three regions of the map are marked to show the possible states of a node. If the occupancy of a cell places it in *region I*, the cell is classified as empty and a maximum conductance is assigned. If the occupancy falls into *region III* the cell is classified as full and the corresponding node is assigned a minimum conductance. *Region II* corresponds to cells neither full nor empty. The graph corresponds to the mapping function given by

$$f(x) = 10.0 \cdot \exp[-0.2(4.0 \cdot x)^{3.05}]. \tag{7}$$

C. Formal Definition and Solution of the System of Equations

Formally, the overall system can be represented as follows.

Consider an environment map M, which contains obstacles of various shapes and sizes. The initial position of the robot is q_0 and the destination point is q_f. Assume a square, bounded region centered about

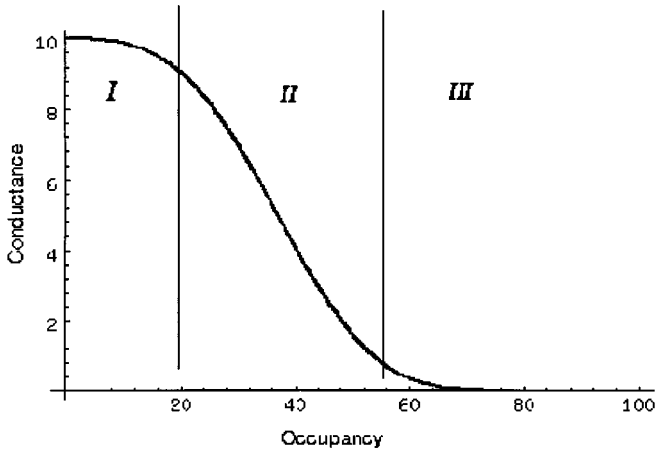

Fig. 2. Resistance mapping function.

q_0 which includes q_f and can be divided into an $n \times n$ grid, X. The grid is discretely represented by the matrix, C, where the value of each entry (the occupancy) is given by c_{ij}, the percentage of the area of the grid cell occupied by obstacles of map M. Mathematically, c_{ij} is given by

$$c_{ij} = \frac{Area(\chi_{ij} \cap M)}{Area(\chi_{ij})} \tag{8}$$

where $\cap$ is geometric intersection.

Consider a resistor network that consists of $n \times n$ nodes of resistors each node containing eight resistors connected in parallel at one point. The free end of each resistor is tied to one resistor from a neighboring node. Let G be a matrix whose entries contain the value of the conductances (inverse of the resistance) of each node of the network. Then the function of (7) is a one-to-one and onto mapping from C to G such that:

$$C \xrightarrow{f(x)} G. \tag{9}$$

Following KCL taken over the entire network, the matrix form of the system of equations is

$$A \cdot V = J \tag{10}$$

where A is an $(n^2 \times n^2)$ matrix, called the admittance matrix; V is an $(n^2 \times 1)$ matrix representing the potential values at each node of the resistor value; and J, the current matrix, is an $(n^2 \times 1)$ matrix whose values are non-zero only at points of application of external current sources (the initial and final points only). The solution to (10) is

$$V = A^{-1} \cdot J \tag{11}$$

and defines the discrete and bounded electrostatic potential field used to determine the navigation path.

The boundaries of the field are defined at the outer cells of the network and at nodes of the network whose corresponding occupancy cell is marked 100% full. To determine a desired direction of travel from the EPF, a vector is associated with each cell connected to the cell containing the MR with magnitude equal to the amount of current flowing through the specified branch. If the resistance between the central node and all of its neighbor nodes is equal, then the potential drop can be used in place of the current. The sum of these vectors is then reported to be the direction of travel along the minimum occupancy path.

D. Global Navigation Function

Rimon and Koditschek proposed a *global navigation function* to specifically force the function used to generate the potential field to have only one local minimum located at the single goal point [11].

Let Ψ be a robot free configuration space, and let q_f be a goal point in the interior of Ψ. A map φ: $\Psi \rightarrow [0,1]$ is a navigation function if it is

1) smooth on Ψ (at least a C^2 function);
2) polar at q_f, i.e. has an unique minimum at q_f on the path-connected component of Ψ containing q_f;
3) admissible on Ψ, i.e., uniformly maximal on the boundary of Φ;
4) a Morse function.

The proposed EPF solution meets the four outlined criteria, and thus, it is a global navigation function. The existence of the first derivative of the electrostatic potential is proven by the fact that $\nabla\phi = (Q_S/\varepsilon)$, where Q_S is the total charge applied through a source. The existence of the first derivative of the potential field demonstrates the smoothness of the function. Combining this result with Gauss's Law shows the existence of the second derivative of the potential field at points of application of external sources. Points of the field that do not have a connected external source have a second derivative of zero satisfying Laplace's equation. Further, a real-valued function on the free configuration space is said to be *admissible* if it is uniformly maximal on the boundary of Ψ, that is, where the robot touches an obstacle

$$V(q)\begin{cases} = c & \forall\, q \in boundary(\Psi) \\ < c & \forall\, q \in inside(\Psi). \end{cases} \tag{12}$$

A boundary of the proposed EPF solution is a node at which the conductance equals zero—when a node is open circuited. Strictly speaking no comment on the potential of not connected points may be offered. But since no current can flow into or out of a not connected node, it is postulated that no path can intersect with the boundary. So the condition is satisfied by the EPF. Further, according to Rimon and Koditschek, it can be shown that trajectories of a dissipative system with admissible potential energy that start with suitable initial velocity remain away from the obstacles. Since the proposed EPF solution is compact, and bounded, a controller obtained from the specified admissible function—Kirchhoff's Laws—is bounded and steers the robot away from the obstacles if some initial speed limit is imposed on the robot. The fourth property is that a navigation function be Morse. A Morse function is one whose Hessian (the matrix of the second derivative) evaluated at the critical points is nonsingular. A simple explanation of a Morse function is that there are no degenerate critical points in the field. Note that the potential function is shown to satisfy Laplace's equation at all points within the field, thus, only saddle points exist at any critical point within the field.

E. Linear Complexity Path Generation

As explicitly shown in [16], the complexity of the occupancy map generation for each polygon is

$$C_{OM}^{(i)} = n_i + size^2(4n_i + I) \tag{13}$$

for a total complexity given by

$$C_{OM} = \sum_{i=1}^{m} n_i + size^2(4n_i + I) \tag{14}$$

where n_i is the number of vertices of the ith polygon of the space, *size* is the dimension of the resistor network (the network has *size* × *size* nodes), and m is the number of polygons in the space. If n_M is assigned to be the maximum number of vertices of any polygon in the space, then it may be asserted that

$$C_{OM} \leq m(n_M + size^2(4n_M + I). \tag{15}$$

All other procedures that follow the occupancy map generation rely only on the fixed dimension occupancy map, operating with a constant complexity, depending only on the size of the resistor network that is fixed at run time. The values of the occupancy map are mapped in a one-to-one and onto mapping to the resistor network. This process is a simple numerical conversion from percentage occupancy to resistance value based on (7). All that is required is a single pass through the occupancy map, resulting in a complexity of

$$C_{IM} = size^2. \tag{16}$$

The solution of the system of equations is done over a sparse representation of the system matrix both before and after the factorization. The complexity of Cholesky factorization using full matrices is found to be $O(N^3)$

$$\begin{aligned} C &= \sum_{i=1}^{N}\sum_{j=1}^{N}\sum_{k=1}^{i-1} 1 = \sum_{i=1}^{N}(N-i)(i-2) \\ &= (N+2)\sum_{i=1}^{N} i - \sum_{i=1}^{N} i^2 - 2N\sum_{i=1}^{N} 1 \\ &= \tfrac{1}{2}(N+2)N(N+1) - \tfrac{1}{6}N(N+I)(2N+I) - 2N^2 \\ &= \tfrac{1}{6}N^3 - \tfrac{3}{2}N_2 + \tfrac{7}{6}N. \end{aligned} \tag{17}$$

Making the system matrix sparse allows one loop to iterate over a constant number much smaller than N. Since the resistor network is a fixed network, the connectivity of each node is the same regardless of the mapping from the environment. Knowing the connectivity, not only can the fill for a solution be predicted, but an optimal ordering for the elimination can be performed off-line and then hardcoded into the calculation of the solution [5], [21], [30], [33]. The complexity of finding the Cholesky factorization of the system matrix including sparsity of the system matrix and with previous knowledge of the created fill (with c_1 and c_2 constants much smaller than N) is of the order of $O(N)$

$$C = \sum_{i=1}^{N} c_1 c_2 = c_1 c_2 N \qquad c_1, c_2 \ll N \tag{18}$$

The complexity of the total solution is the summation of (16)–(18)

$$\begin{aligned} C &= C_{OM} + C_{IM} + C_S \\ &= mn_M + m(4n_M + 1)size^2 + 3size^2 + size. \end{aligned} \tag{19}$$

Removing the non-variable terms, this reduces to $O(mn_M)$ which is linear with respect to the variables, the number of polygons in the space, m, and the maximum number of sides of any polygon, n_M.

IV. Similarity to Dynamic Programming

The Dynamic Programming (DP)-based approach to the shortest path finding problem is divided into the sub-problems of finding the next step plus finding the rest of the path with the total cost given by the general expression [21], [24], [30]

$$C(u,v) = c(u,v) + c(v,f) \tag{20}$$

where u is the present node, v is the next step, and f is the final destination. The EPF-based solution may also solve the problem in a similar manner. Ohm's Law determines the electric current of a path as the product of the potential and the conductance

$$I(u,f) = \phi(u,f) \cdot g(u,f). \tag{21}$$

When tracing a path through a resistor network from node u to node f the path takes an initial step through only node v. After node v, the path degenerates into a sequence of series and parallel branches (resistances). The overall conductance of the path can be split accordingly

$$I(u,f) = \phi(y,f) \cdot [g(u,v) + g(v,f)]. \tag{22}$$

The total amount of current that flows through a path remains constant due to the conservation of energy principle associated with a closed electric circuit. When current in a path encounters parallel branches, the current is split between the branches according to the conductive strength of the branches. Since the path from u to f is initiated only through node v, there is no current split; thus, $I(u,f)$ can be seen entirely in the branch current of $I(u,v)$

$$I(u,v) = I(u,f) = \phi(u,f) \cdot [g(y,v) + g(v,f)]. \tag{23}$$

Anywhere in the resistor network, the current at each step reflects the conductance of the immediate branch, $g(u,v)$, and the effective conductance of the rest of the network, $g(v,f)$, along the path.

Both DP and EPF algorithms require knowledge of the immediate next step, as well as complete knowledge of the rest of the path. A dynamic programming algorithm recursively solves for the remainder of the path, while the EPF algorithm utilizes the complete system of equations to solve for the effective cost of the remainder of the path. Dynamic programming algorithms, backtracking algorithms, and the EPF algorithm all guarantee a shortest path approach. Both the DP and backtracking algorithms operate with a complexity magnitude of $O(n^2)$, n is the number of nodes in the network. As previously justified, the basic EPF solution may also be implemented to operate with $O(n^2)$ magnitude; recall that the variable N is the size of the system matrix which is $N \times N$, or equivalently $n^2 \times n^2$.

V. Simulation and Experimental Results

Both simulation and experimental (real-time) results are presented and several implementation issues are discussed. The proposed navigation system has been implemented on the *Nomad 200* robot using the *Cognos* development software package that provides a communication link with the actual mobile robot [15]. It is mentioned that results resemble experimental results as explicitly shown in [16] for most case studies.

In a completely static environment, the EPF planner may generate a complete path through a known environment in a single iteration; the generated path is guaranteed to be approximately optimal (minimum total occupancy) at the given cell resolution level. However, as the robot moves closer to the desired goal point, the path may be re-generated given a different cell resolution, if necessary. On the other hand, in a dynamic environment, the EPF is recalculated at each sampling time (that varies according to the cell resolution); when this is the case, only the next step of the approximately optimal path is generated. In a dynamic environment the EPF takes into account the previous path changes in every iteration. In this manner, the dynamic environment is reduced to a sequence of static snapshots (during one sampling time interval). Results are presented next. Comments, justifications and discussion are given when necessary.

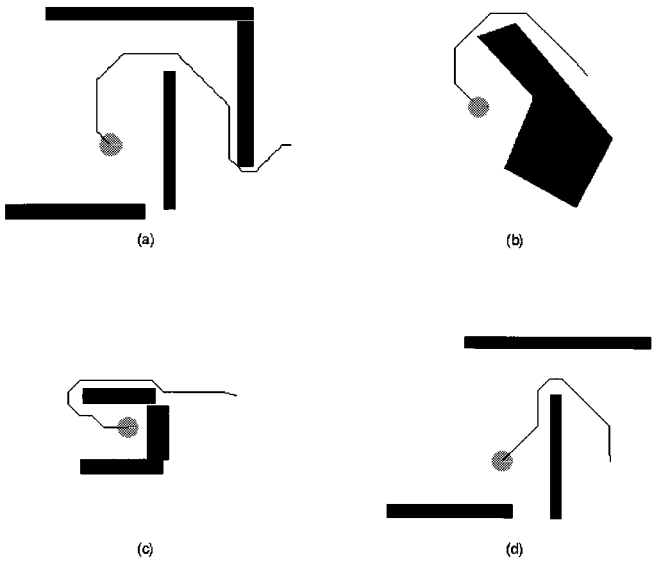

Fig. 3. Simulation test case 1 in four different static environments.

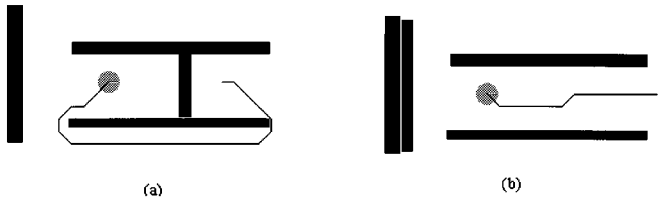

Fig. 4. Simulation test case 2 in two different static environments.

A. Simulation Results

Figs. 3–5 show simulation runs in several static environments demonstrating the inclination of the EPF approach to maximize the distance from the obstacles as the robot is driven along the path. In these three simulation test cases, the environment was broken into squares 110 × 110 pixels, corresponding to 11 × 11 in in the environment. The effect of this imposed minimum resolution is seen especially in Fig. 4(b). As the vehicle is attempting to move down a straight hallway, the initial move is to center the robot, however, due to the minimum resolution, the path overshoots and is not actually centered between the two walls. Further, note that the occupancy value of any cell corresponds to a single value representing the percent of the cell filled by obstacles. In the case of binary mapping, all that is known is that an object resides within the cell. Small obstacles in the environment may be poorly represented, thus causing the generated path to pass very close to the obstacle. In both cases of Fig. 5, the obstacles are larger than the resolution of a single cell; thus oscillatory behavior is almost non existent. The paths taken in these two examples demonstrate the increase in effectiveness of the EPF solution as the environment becomes more cluttered. The path of Fig. 5(b) is a very smooth path that approaches the goal at all times.The path taken by the robot at each point can be seen to maximize the distance from all close obstacles. The path of Fig. 5(a) also attempts to maximize the distance from the obstacle.

Fig. 6 demonstrates the ability of the EPF path planner to navigate long hallways. The MR is shown at the end of the path. The path of Fig. 6(b) after the robot has reached the center hallway appears to show some discrepancy when compared with the path of Fig. 6(a). The sinusoidal path at the beginning of the path of Fig.6(b) is due to a high cell resolution. Since the goal point is far away, each cell contains less information about the walls of the environment, slightly modifying the

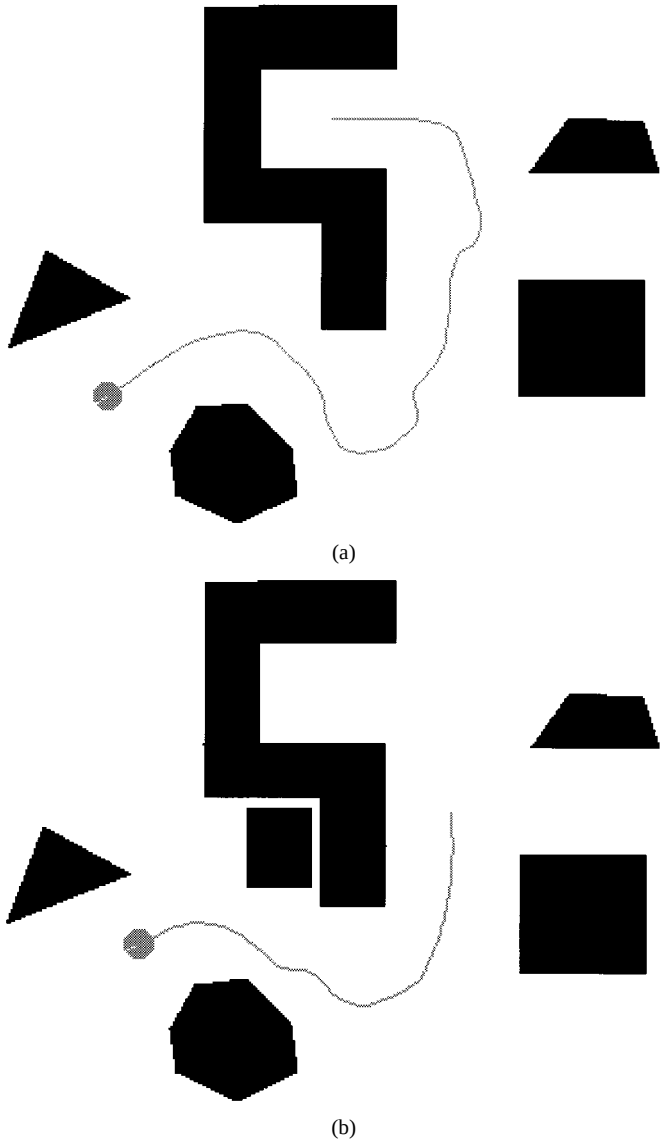

Fig. 5. Simulation test case 3 in two slightly different static environments.

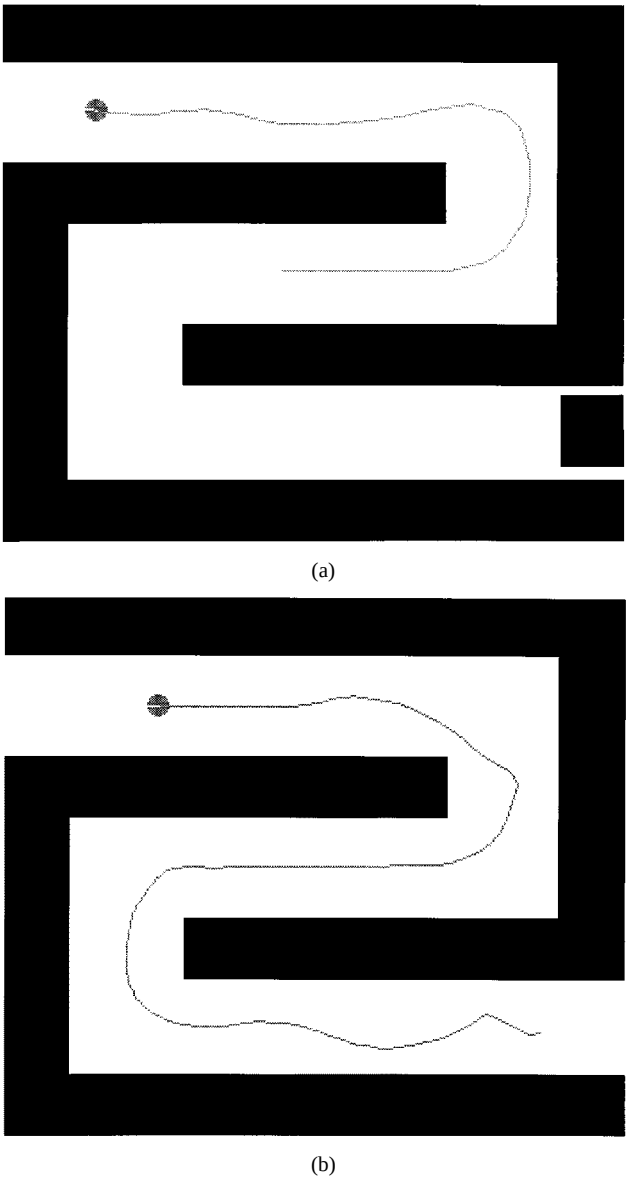

Fig. 6. Test case 4: two paths generated in a simulated hallway environment.

path. As the robot moves closer to the wall, the occupancy of the cells close to the robot increases and forces the robot to rebound off the wall slightly. This effect is seen in many of the test studies when the resolution is very large compared to the size of the obstacles.

Fig. 7 demonstrates the case of a dynamic environment with a hidden obstacle, and at the same time provides the clearest justification for an on-line global path planner. The motion of the obstacle begins when the robot reaches point A, and it slides into its final location. In this case, it is assumed that the EPF path planner has complete knowledge of the dynamic object, including its velocity vector. This allows the robot to completely avoid the "blocked" area. With less precise information about the moving obstacle, the path taken is much less ideal than the one shown in this test case. In some simulation runs, when the dynamic obstacle was completely unknown, the potential field avoided the area as long as the sonar sensors identified the obstacle. Once the sonar sensors lose sight of the obstacle, the potential field "forgets" about the obstacle and attempts to plan a path through the gap of the two objects. While the sonars detected the obstacle, if the EPF planner pushed the robot far enough around the seven-sided obstacle, the path planner planned around the obstacle avoiding the area of the moving

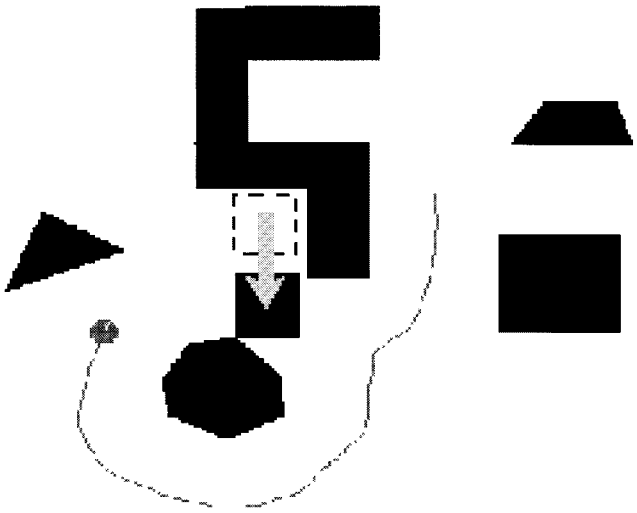

Fig. 7. Simulated dynamic environment test case 5.

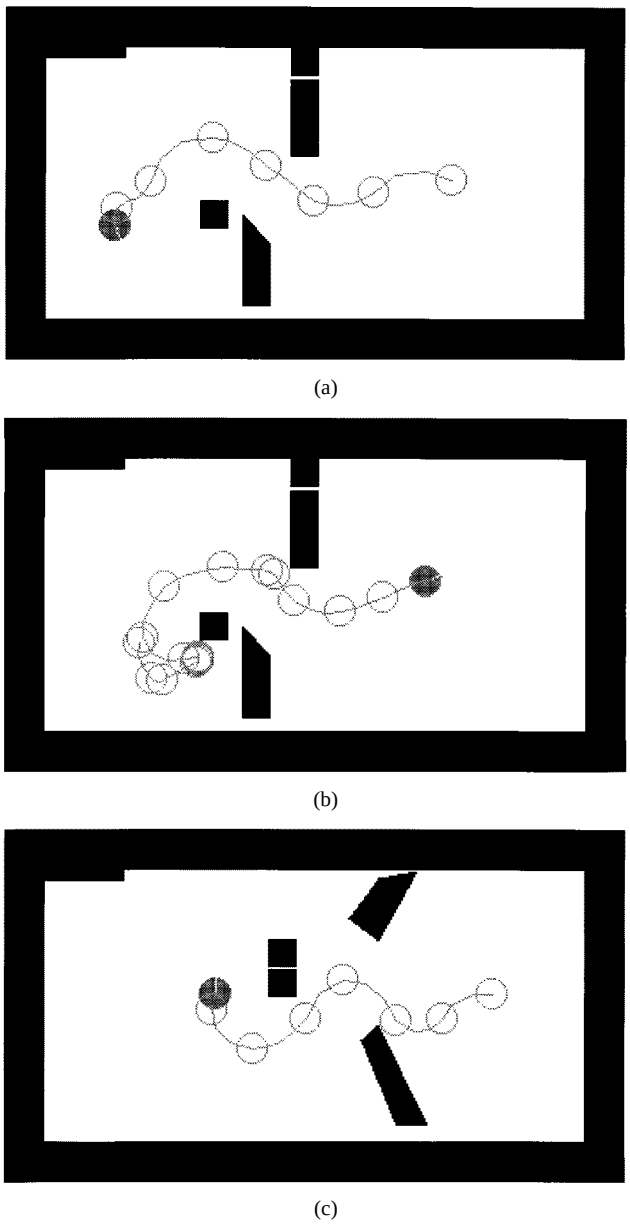

(a)

(b)

(c)

Fig. 8. The results of three different, real-time test runs.

object. Observe that with knowledge of the overall structure of the environment the EPF approach directs the robot to move not necessarily in the direction of the goal, but in the direction which generates the most efficient path to the goal. The EPF approach, knowing that the dynamic obstacle will block the intended path has enough time to modify the path and completely avoid the area of the moving obstacle. Complete knowledge of the environment is unlikely in dynamic situations, making this particular behavior more of an ideal than a reality and not suitable in rapidly changing environments.

B. Experimental Results

Real-time experimental results have been obtained using the *Nomad200* in a laboratory environment. The room is a clean environment with rectangular obstacles and measures approximately 300 in by 150 in. The grid size used to calculate the EPF-based path was set to be 13 × 13 giving a sampling rate of approximately 1 s. (Note that a grid size of 11 × 11 reduces the sampling rate to approximately 0.65 s.) The objects were placed in the room, their position measured and the result placed in a map, which can be viewed by the *Cognos* software package. The robot is localized within the room before each test run. The position of the robot is recorded at regular time intervals and the subsequent path is displayed through the *Cognos*'s GUI. During

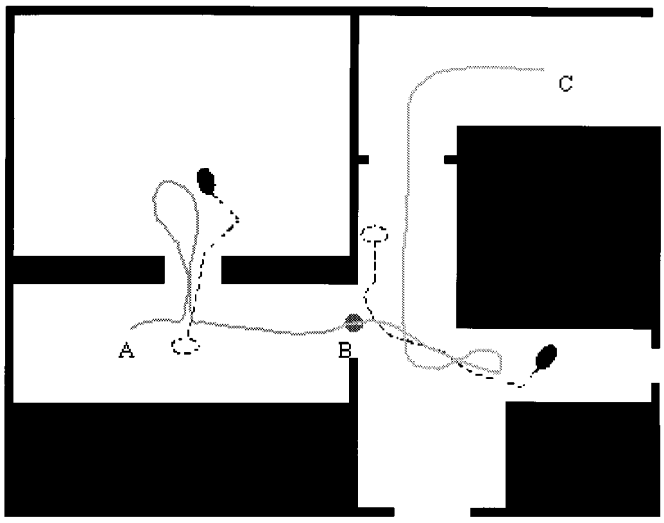

Fig. 9. Experiment in a realistic structured environment with moving obstacles.

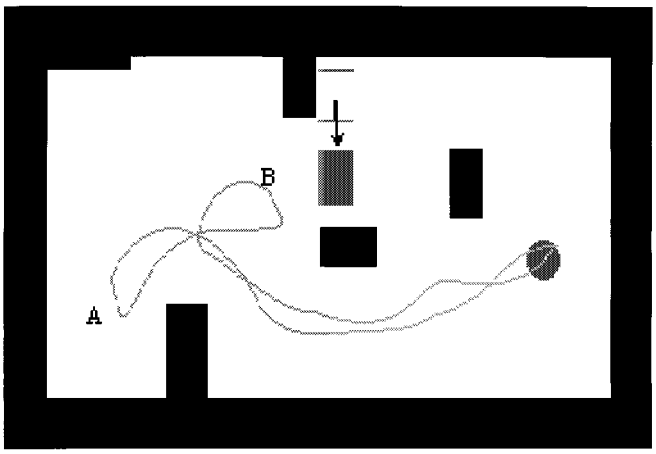

(a)

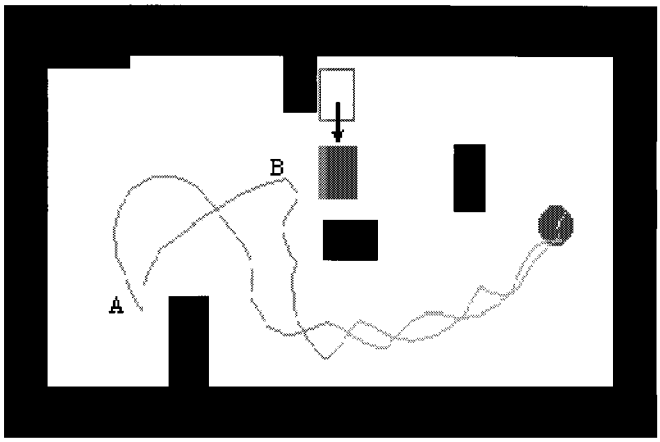

(b)

Fig. 10. Navigation in the same environment. (a) Simulated and (b) real time results.

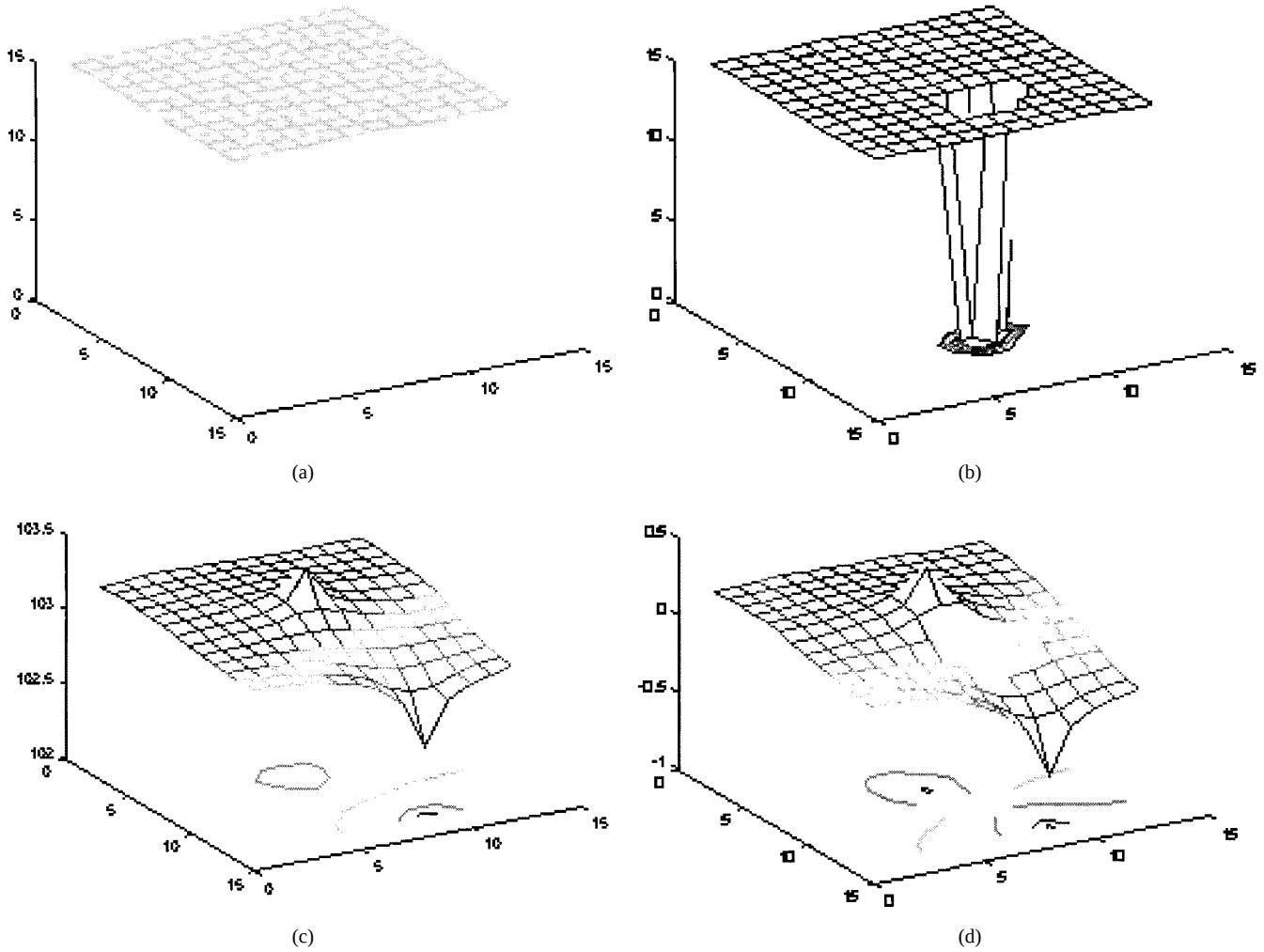

Fig. 11. Occupancy map and potential field of two different environments. (a) is the occupancy map whose solution is shown in (c), and (b) is the occupancy map whose solution is shown in (d). A contour mapping of the potential fields of (c) and (d) reflect the position of equipotential surfaces in the field.

the test executions, all programs were run, under the *Linux* operating system, directly on the main processor of the robot, a Pentium 133. Fig. 8 displays three different, real-time runs of the EPF solution. The paths displayed show the robot as the solid circle at the end of the traversed path. The circles along the path show the robot's position at regular intervals. In all experimental runs, the robot completed the run from the initial position to the desired end point with no collisions. No localization module was used with these test runs.

The testbed shown in Fig. 9 is the actual overall floor plan of our laboratory facility. The robot starts from point A and the final destination is point C. Moving obstacles, humans in this case, force the robot to divert from its path. Obstacles' trajectories are represented with the dashed line, while the robot's trajectory is represented with the red line. The robot reaches the goal point avoiding collisions.

Fig. 10 compares the navigation results using the *Cognos* simulation package and the *Nomad 200* robot, for the same test case (environment, goal points, and initial position). The initial and final positions are the same with a single intermediate goal point located at point A. As the robot tracks to the final position; it attempts to pass between the obstacle in the middle of the room and the uppermost obstacle. As the robot reaches point B of the path, a hidden obstacle (a human in the experimental case) moves to block the path of the robot with a speed roughly equivalent to the speed of the robot. The potential field knows neither the presence nor the velocity vector of the obstacle *a priori*.

C. Discussion

The effect of different parameters within the occupancy map and the resulting effect on the potential field are explicitly shown in Figs. 11 and 13. Fig. 11(a) shows the occupancy map of an environment devoid of obstacles. The resulting potential field of Fig. 11(c) demonstrates the resulting potential field used to generate the optimal path. A single obstacle is inserted into the environment of Fig. 11(b). The potential field generated for this mapping is shown in Fig. 11(d). In the figure of the potential field, the lines in the XY-plane represent a contour drawing of the potential field corresponding to equipotential surfaces within the field.

All paths will move from one line to the next in the direction of the tangent of the line. The intensity of the lines in the figure represents the relative speed of the negative descent of the potential field. Areas of the occupancy map that contain obstacles are represented as depressions within the field. Thus, the flat surface at the top of the occupancy field represents the free space of the environment.

Fig. 12 demonstrates the effect of resolution on the occupancy and subsequently on the potential field. The physical area of the environment to be mapped into a single cell of the occupancy map is determined by the relative distance of the initial position and the goal position. A larger resolution of the cells implies that less information is represented per cell of the occupancy map. However, a larger area of

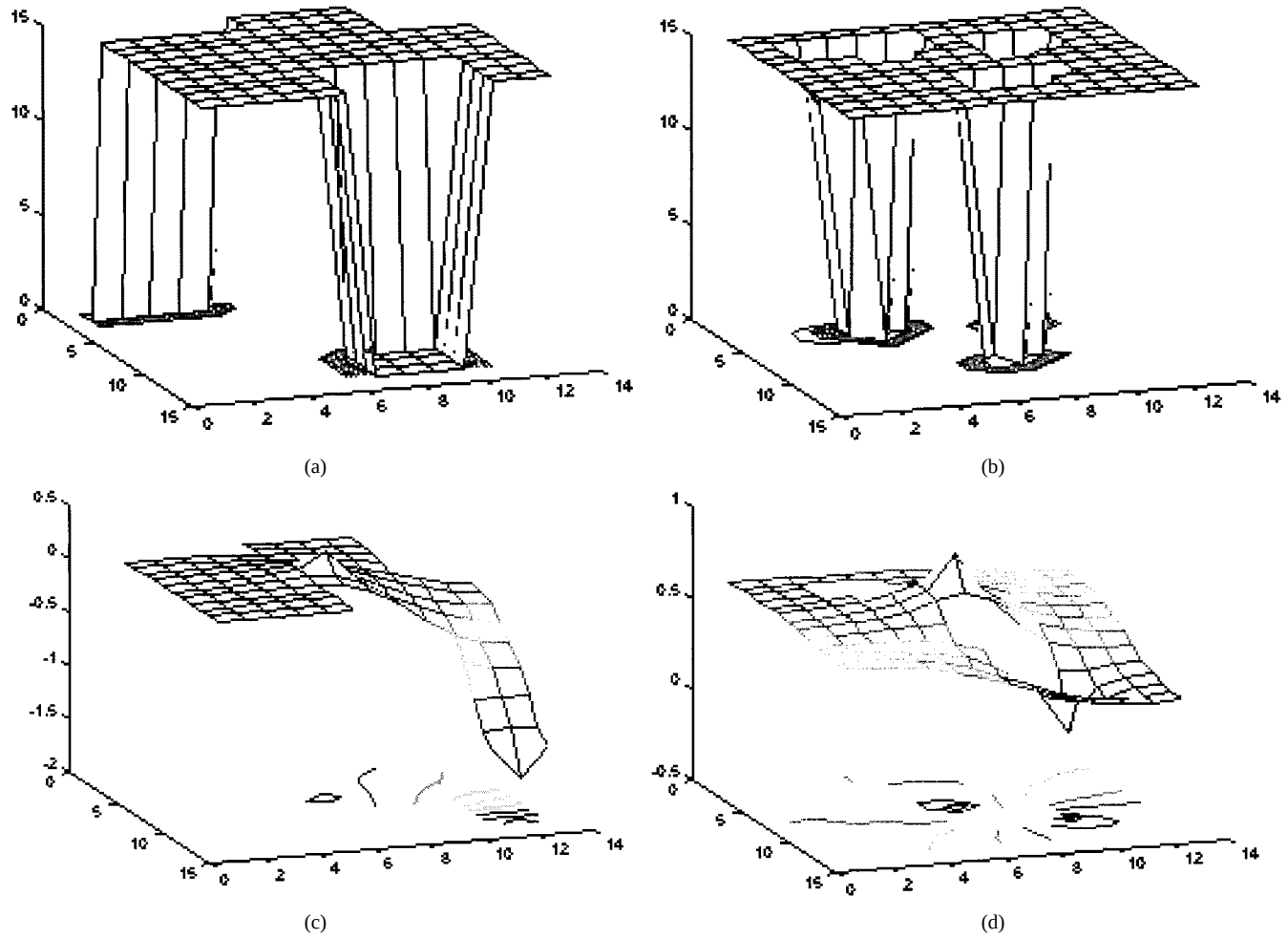

Fig. 12. Two different mappings, and related potential field, of the same environment. The resolution of the occupancy map reflected in (a) is smaller than the resolution of the cells of the occupancy map in (b). The availability of more paths in the potential field of (d) as compared to the field of (c), reflects the increased area covered by the mapping. The contour lines of (c) and (d) reflect the equipotential surfaces of the respective potential field.

the environment can be represented. If the goal point is near the edge of a map with a certain resolution, increasing the resolution will move the goal point to a cell which is more central to the map, allowing more paths to be potentially generated. In Fig. 12, the additional paths are especially seen in the contour lines of the potential field of Fig. 12(d). Fig. 12(a) is the occupancy map, which corresponds to the potential field of Fig. 12(c), and Fig. 12(b) is the map which corresponds to the potential field of Fig. 12(d).

Another method to incorporate more of the environment into the occupancy map, and thus into the solution space of the potential field, is to increase the size of the grid. As more cells are added to the grid, more of the environment can be represented without changing the resolution of the current cells. When deciding the desired size of the grid the desired time of computation should be considered. Even though the computational complexity for the solution of the potential field is a constant, and thus does not show in the overall computational complexity, the majority of the runtime of the process is consumed through the calculation of the solution of the resistor network. Thus, a resistor grid which is very large would take an inordinate amount of time to solve, negating any advantage gained through increasing the size of the grid.

VI. Conclusions

The proposed potential field follows the natural laws of electrostatics to build a single EPF represented discretely as a lumped element resistor network. A single metric, resistance, reflects both the distance to the goal and the presence of obstacles. A system of linearly independent equations is solved to generate two related fields, the scalar potential field and the vector current field. Tracing a path of maximum current flow through the branches of the network is equivalent to tracing a path of minimum resistance that maps to a minimum occupancy path.

Minimizing area occupancy along a navigation path inherently incorporates two important navigation constraints: minimize the distance traveled and avoid collisions with obstacles. Since the optimum path minimizes the sum of swept occupancies, a straight-line path gives a minimal occupancy path in an area without obstacles. An obstacle in the environment not only effects the immediate cells of the resistor network; the resistances of all regions of the network are affected. Completely occupied cells of the network are modeled as an infinite resistance, or more simply put as an open circuit. Thus, the optimum path, seeking to minimize the total occupancy of the path, is pushed away from the boundary of obstacles, yet is attracted towards the goal position.

The "occupancy" optimization criterion has several advantages over a simple distance criterion. A distance optimization criterion, or cost function, cannot be variable—the distance between any two points is fixed. Thus, no other allowances can be incorporated into the cost function. On the other hand, the occupancy of a cell describes the volume of obstacles in the environment, or the smoothness of the ground in the environment, or any combination of quantities that may effect the quality of the path through the area of the environment.

The result of the EPF solution is a minimum occupancy path. The immediate next step plus the rest of the path determine the complete path. The network resistance of the rest of the path is an effective resistance; it is the series and parallel combination of all connected nodes between the next step and the goal point. A very low resistance cell in parallel with a very high resistance cell will average out to a medium resistance path. An averaging happens as the resistor network's system of equations is solved. Within a long hallway, the effective resistance of the space immediately next to the two walls is highest. The effective resistance between the two walls forms a trough with the lowest point the exact center of the hallway. A robot following the path of lowest resistance through the hallway tends to center itself in the hallway; in effect, maximizing the distance from all obstacles in the immediate environment. This affect is seen between any grouping of objects through which the EPF path goes.

REFERENCES

[1] D. Cheng, *Field and Wave Electromagnetics*. Reading, MA: Addison-Wesley, 1989, ch. 2nd ed.

[2] J. Cross, *Electrostatics: Principles, Problems, and Applications*. Bristol, U.K.: Adam Hilger, 1987.

[3] C. Desoer and K. Kuh, *Basic Circuit Theory*. Tokyo, Japan: McGraw-Hill KogaKusha, Ltd., 1969.

[4] J. Irwin, *Basic Engineering Circuit Analysis*. New York: Wiley, 1990.

[5] D. Stinson, *An Introduction to the Design and Analysis of Algorithms*. Winnipeg, Alta, Canada: Charles Babbage Res. Center, 1987, ch. 2nd ed.

[6] M. Alwan, P. Cheung, A. Saleh, and N. C. Obeid, "Combining goal-directed, reactive and reflexive navigation in autonomous mobile robots," in *Proc. Australian-New Zealand Conf. Intelligent Information Systems*, 1996, pp. 247–250.

[7] J. C. Latombe, *Robot Motion Planning*. Norwell, MA: Kluwer, 1991.

[8] I. Connolly and J. B. Burns, "Path planning using Laplace's equation," in *Proc. IEEE Int. Conf. Robotics and Automation*, vol. 3, 1990, pp. 2102–2106.

[9] Y. K. Hwand and N. Ahuja, "A potential field approach to path planning," *IEEE Trans. Robot. Automat.*, vol. 6, no. 1, pp. 23–32, 1992.

[10] Y. Kitamura, T. Tanaka, F. Kishino, and M. Yachida, "3-D planning in a dynamic environment using an doctree and an artificial potential field," in *Proc. IEEE Int. Conf. Intelligent Robots and Systems*, vol. 2, 1995, pp. 474–479.

[11] E. Rimon and D. Koditschek, "Exact robot navigation using artificial potential functions," *IEEE Trans. Robot. Automat.*, vol. 8, no. 5, pp. 501–518, 1992.

[12] Y. Zhang, "Sensor-Based Potential Panel Method for Robot Motion Planning," Ph.D. dissertation, Univ. Southwestern Louisiana, 1995.

[13] J. O. Kim and P. Khosla, "Real-time obstacle avoidance using harmonic potential functions," *IEEE Trans. Robot. Automat.*, vol. 8, no. 3, pp. 338–349, 1992.

[14] G. Oriolo, G. Ulivi, and M. Vindittelli, "Real-time map building and navigation for autonomous robots in unknown environments," *IEEE Trans. Syst., Man, Cybern.*, vol. 28, no. 3, pp. 316–333, 1998.

[15] Nomadic Technologies, Inc., *Nomad 200: User's Manual: Software Vers. : 2.6*, 1996.

[16] T. Hebert, "Navigation of an Autonomous Vehicle Using a Combined Electrostatic Potential Field/Fuzzy Inference Approach," Ph.D. dissertation, Univ. Southwestern Louisiana, 1998.

[17] Y. Zhang and K. P. Valavanis, "Sensor-based 2-D potential panel method for robot motion planning," *Robotica*, vol. 14, pt. 1, pp. 81–89, 1996.

[18] ——, "A 3-D potential panel metehod for robot motion planning," *Robotica*, vol. 1, pt. 5, pp. 421–434, 1997.

[19] T. Asano, L. Guibas, J. Hershberger, and H. Imai, "Visibility of disjoint polygons," *Algorithmica*, vol. 1, pp. 46–63, 1986.

[20] E. Welzl, "Constructing the visibility graph for n line segments in $O(n^2)$ time," *Inform. Process. Lett.*, vol. 20, pp. 167–171, 1985.

[21] M. Fredman and R. Tarjan, "Fibonacci heaps and their uses in improved network optimization algorithms," *J. ACM*, vol. 34, no. 3, pp. 596–615, 1987.

[22] S. Ghosh and D. Mount, "An output sensitive algorithm for computing visibility graphs," in *Proc. 28th IEEE Symp. Foundations of Computer Science*, 1987, pp. 11–19.

[23] "Shortest Paths in Euclidean Paths in Euclidean Space with Polyhedral Obstacles, TR-05-85," Brandeis Univ., 1985.

[24] "Planning Shortest Paths, Research Report 561," Stanford Univ., 1986.

[25] H. Rohnert, "Shortest paths in the plane with convex polygonal obstacles," *Inform. Process. Lett.*, vol. 23, pp. 71–76, 1986.

[26] J. T. Schwartz and M. Sharir, "On the 'piano movers' problem I: The case of a two-dimensional rigid polygonal body moving amidst polygonal barriers," *Commun. Pure Appl. Math.*, vol. 36, pp. 345–398, 1983.

[27] A. Van der Stappen, D. Halperin, and M. Overmars, "Efficient algorithms for exact motion planning amidst fat obstacles," in *Proc. IEEE Int. Conf. Robotics and Automation*, 1993, pp. 297–304.

[28] D. Leven and M. Sharir, "An efficient and simple momtion planning algorithm for a ladder moving in 2-dimensional space amidst polygonal barriers," in *Proc. 1st ACM Symp. Computational Geometry*, 1985, pp. 211–227.

[29] F. Avnaim, J. Boissonnat, and B. Faverjon, *Proc. IEEE Int. Conf. Robotics and Automation*, 1988, pp. 1656–1661.

[30] L. Helms, *Introduction to Potential Theory, Pure and Applied Mathematics*. New York: Academic, 1969.

[31] J. Hutchinson, C. Koch, J. Lea, and C. Mead, "Computing motion using analog and binary resistive networks," *IEEE Comput. Mag.*, vol. 21, pp. 52–63, 1988.

[32] J. Kim and P. Khosla, "Real-time obstacle avoidance using harmonic potential functions," in *Proc. IEEE Int. Conf. Robotics and Automation*, 1991, pp. 790–796.

[33] S. Pissanetzky, *Sparse Matrix Technology*. New York: Academic , 1984.

[34] J. Reif, "Complexity of the mover's problem and generalization," in *Proc. 20th Symp. Foundations of Computer Science*, 1979, pp. 421–427.

[35] L. Singh, J. Wen, and H. Stephanou, "Motion planning and dynamic control of a linked manipulator using modified magnetic fields," in *Proc. IEEE Int. Conf. Robotics and Automation*, 1997, pp. 1142–1147.

[36] L. Tarassenko and A. Blake, "Analogue computation of collision-free paths," in *Proc. IEEE Int. Conf. Robotics and Automation*, 1991, pp. 540–545.

[37] L. Tarassenko, M. Brownlow, G. Marshall, and J. Tombs, "Real-time autonomous robot navigation using VLSI neural networks," *Advances in Neural Information Processing Systems*, pp. 422–428, 1991.

[38] J. F. Canny and J. H. Reif, "New loer bound techniques for robot motion planning problems," in *Proc. 28th IEEE Symp. Foundations of Computer Science*, 1987, pp. 49–60.

[39] R. C. Arkin, *Behavior Based Robotics*: MIT Press, 1998.

[40] J. H. Reif and M. Sharir, "Motion planning in the presence of moving obstacles," in *Proc. 25th IEEE Symp. Foundations of Computer Science*, 1985, pp. 144–154.

[41] J. T. Schwartz and M. Sharir, "On the 'piano movers' problem II: General techniques for computing topological properties of real algebraic manifolds," *Adv. Appl. Math.*, vol. 4, pp. 298–351, 1983.